3606 *Macromolecules* **2010**, *43*, 3606–3612
DOI: 10.1021/ma100191d

Macromolecules
ARTICLE

Formation of Homooligosaccharides Using Base-Promoted Glycosylation of Unprotected Glycosyl Fluorides

Andreas Steinmann,† Julian Thimm,† Martin Matwiejuk, and Joachim Thiem*

Faculty of Science, Department of Chemistry, University of Hamburg, Martin-Luther-King-Platz 6, D-20146 Hamburg, Germany. †These authors contributed equally

Received January 26, 2010; Revised Manuscript Received February 15, 2010

ABSTRACT: Homooligomeric saccharides are of general interest with potential applications in chemical, pharmaceutical, and food industry as well as for materials with novel properties. This contribution describes a methodology of a base-promoted "single step self-oligomerization" of glycosyl fluorides as donors leading to oligomers with up to ~25 saccharide units. The influences of base and reaction time were examined. Linkage analysis of the corresponding alditol acetates by GC/MS allowed for calculation of average structural elements of oligomers.

Introduction

Commonly used approaches for glycosylation reactions use mainly activated and protected glycosides in a "step by step" fashion. There is a limited number of higher glycosylation or multiple glycosylation reactions, and to date there are only a couple of examples of carbohydrate-based syntheses of oligomers (Scheme 1).[1−3]

Recently, high regio- and stereoselectivity was achieved by enzymatic glycosylations of unprotected glycosyl fluorides.[4] The present paper describes a simple synthetic methodology of a base-promoted anionic self-glycosylation of unprotected glycosyl fluorides. Glycosyl fluoride derivatives are attractive donors for the synthesis of oligosaccharides due to activation of their C−F bond by Lewis acids such as e.g. $SnCl_2$, TiF_4, $AgClO_4$, and $BF_3 \cdot Et_2O$.[5−7]

The idea was to polymerize less reactive donors such as glycopyranosyl fluorides (e.g., glucopyranosyl, mannopyranosyl, galactopyranosyl, and fucopyranosyl fluorides) aiming to prevent hydrolysis and decomposition. Because of the well-known reduced reactivity of glycopyranosyl fluorides, there were only a few early examples reported in glycosylation reactions.[8]

Introduction of titanium tetrafluoride and trifluoromethane trimethylsilane fluorophile catalysis initiated wider applications of glycosyl fluorides in glycosylation reactions.[9]

Besides the hydrofluoric cleavage of sugar polymers such as starch and cellulose in liquid hydrofluoric acid, a variety of preparation methods for glycosyl fluorides are established today, and glycosyl fluorides are synthesized with ease.[10] Starting from the unprotected carbohydrate in three steps the glycopyranosyl fluorides are readily accessible.

Initially, the β-pentaacetate is prepared and subsequent fluorination using a solution of hydrofluoric acid in pyridine (70%) leads to the α-glycopyranosyl fluoride exclusively.[11,23] Subsequent Zemplén deacetylation at 0 °C resulted in the desired unprotected glycosyl fluoride (Scheme 2).

For oligomerization the unprotected glycopyranosyl fluoride was dissolved in *N*,*N*-dimethylformamide, and the base promoter such as sodium hydride or lithium hydride was added. Depending on the sugar configuration, the influence of equivalents base promoter used might vary for best results.[12,13]

*Corresponding author. E-mail: thiem@chemie.uni-hamburg.de.

Scheme 1. Example of Protecting Scheme-Controlled Oligosaccharide Synthesis Using Fluorinated Glycosyl Donors and Thiophenyl-Activated Glycosyl Acceptors

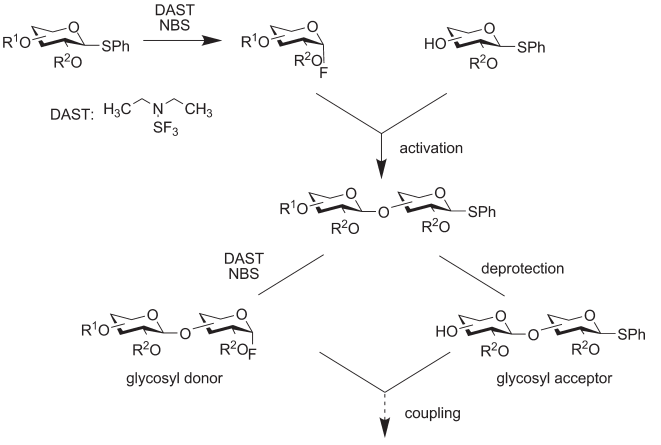

Formation of the alcoholate was done under a slight vacuum at 0 °C in order to promote complete conversion by removal of the generated hydrogen without any oligomerization. In our experiments lithium hydride was favored as a promoter since the harder cation is expected to show higher affinity to the fluoride anion for better activation. This facile preparative approach resembles Schmidt et al.'s "anomeric *O*-alkylation" method, in which an alcoholate substitutes a leaving group at the acceptor (Scheme 3).[12−15] The conceptual difference is that Schmidt et al. activate a partially benzylated oxyanion donor, whereas in our approach this concept was reversed by employing the oxyanion-activated acceptor.

Analysis and Discussion

The molecular weight distribution of the reaction mixtures of the glyco oligomers were analyzed using MALDI-TOF employing either unprotected, peracetylated, or permethylated species. Small fractions of the oligomer mixtures were subjected to methylation analysis (methylation, hydrolysis, and sodium borodeuteride reduction followed by peracetylation) with subsequent GC/MS separation and detection of the corresponding partially

 Published on Web 03/17/2010

Scheme 2. Preparation of Unprotected α-D-Glycopyranosyl Fluorides (5−8)

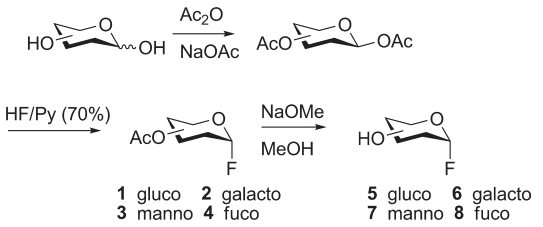

Scheme 3. Glycosylation Concepts of Donor Activation (Left) and Acceptor Activation (Right)[a]

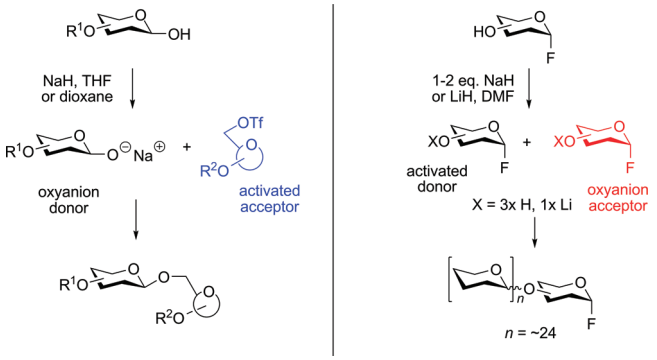

[a] Left: R. R. Schmidt's "anomeric *O*-alkylation" in which glycoside formation of benzyl-protected pyrano and furanoside donors proceed under base promotion by initial oxyanion formation and reaction with triflate activated acceptors.[14] Right: self-oligomerization of unprotected glycosyl fluorides (activated donor). The acceptor is generated *in situ* as an oxyanion using 1−2 equiv of NaH/LiH.

methylated alditol acetates.[16,17] Each resulting alditol carries a particular and characteristic regiospecific methylation and acetylation pattern, which allows to determine the linkages within the polymer (Figure 1). Separation and quantification of methylated alditol acetates was achieved due to differences in their GC retention time and their specific MS fragmentation, hence allowing fingerprint identification.

Exemplary, a MALDI-TOF of the permethylated galactopyranosyl oligomer mixture is shown (Scheme 4). Oligomers up to ~25-mers were detected; however, the presence of even higher oligomers is unlikely, since products with increased molecular weights and functions could not or barely be detected by MALDI-TOF and was supported by GPC analytic (Figure 3). A typical exponential decay for broadly distributed oligomers was observed and represents an artifact of the detector.

Termination units as well as branched building blocks are detected and quantified by GC signal integration. This analytic permits the characterization of structural features of the formed polymers, such as branching and linkage type. The analytical principle is exemplary shown for a mixed octasaccharide (Scheme 5).

Initially, the progress of the oligomerization was examined by sampling fractions over time (20 min, 1 h, 2 h, 4 h, and 22 h).

Scheme 6 shows exemplary a summary of the results of the linkage analysis for each sampling period in the presence of 1 equiv of lithium hydride for glucopyranosyl fluoride **5**. The linkage type vs the relative occurrence in percent (integration over all detected signals) is shown. On the basis of the assumption that initially all regioisomeric alcoholates are formed, all regioisomeric glycosides were expected to be formed and that was indeed confirmed by GC/MS. Differences in the reactivity for each position, e.g. primary > secondary, were observed for the 1→6-branched structural element, which occurs up to 40−50% in the mixture. As evident from the data, it is observed that with

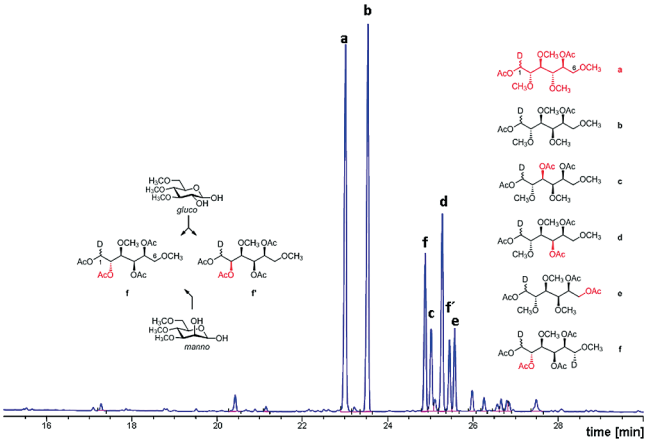

Figure 1. Exemplary GC chromatogram of alditol acetates. Relative ratios of individual peaks are calculated based on the sum of all detected species. MS fragmentation for identification of alditol acetates is not shown. Alditol acetates **f** and **f′** are derived either from *gluco*- and **f** as well from *manno*pyranoses.[12,13,16,17]

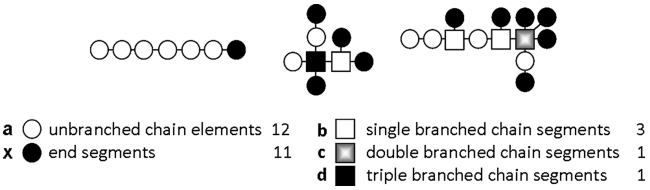

Figure 2. Considerations of chain element counts for an exemplary saccharide mixture in order to calculate an average polymer chain length. Note: unbranched refers here to a minimum of one bond in order to be attached to the chain and is therefore not counted.

Scheme 4. MALDI-TOF of Galactopyranosyl Oligomers[a]

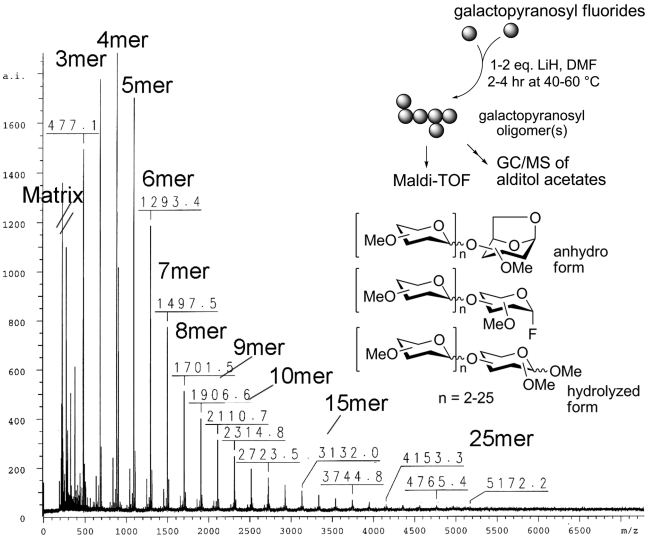

[a] Up to 25-mers were detected after permethylation. The reducing terminal glycosyl residues after methylation might be present in the anhydro, hydrolyzed, or glycosyl fluoride form.

prolonged time 1→6-linkages increase up to 70%, leading to more linear type polymers. The influence of the amount of base promoter with respect to homooligomerization was discussed previously using a random glycosylation approach.[12,13]

Theoretical Considerations

The combined analytical data permit a calculation of an "*average branched structural element*" for each system.[18−20] Even

though the real structure(s) differ from such calculated *average structures*, these considerations are important as they provide insights into the degree of oligomerization and the mechanism, which might allow for improved reaction control.

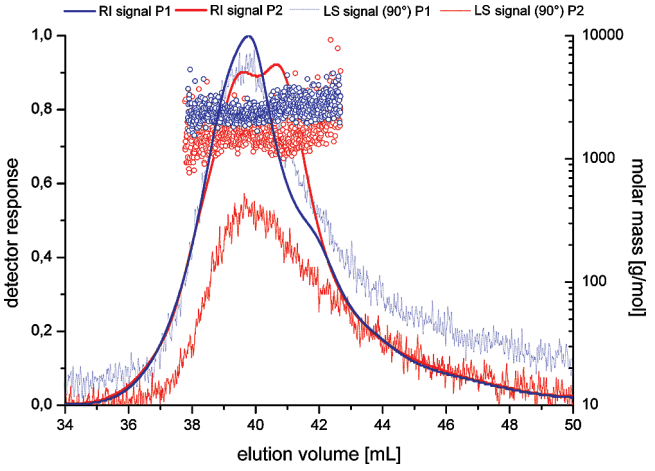

Figure 3. Refractogram for single and double pass glucopyranosyl oligomerization. The plot shows the detector response (refraction index, RI; light scattering at 90°, LS for single pass (P1; 2000−3000 g/mol) and double pass (P2)) proportional to the molar mass of oligomers (1000−3000 g/mol). The second oligomerization pass shows a slight depolymerization, which was not further investigated.

A close look at the results for the presence of linkage types indicates the important observation, that with increased branching the number of terminal units increases and therefore directly correlates to the type of branching. This can be illustrated by an exemplary calculation of an *average chain length* based on three model structures (Figure 2). In this example, three structures of varying chain length of 7-, 8-, and 13-monomer building blocks are illustrated, showing different degrees of branching and linkages (Figure 2). In total, there are 28 monomer building blocks: *12* of them are unbranched, *11* of them are terminal units, *3* are single branched, *1* is double branched, and another *1* is a triple branched monomer.

The following formula was derived to calculate an average chain length:

$$\text{average chain length } \overline{\text{CL}} = \left[\frac{x+a+b+c+d}{x-b-2c-3d}\right] = \left[\frac{100}{x-b-2c-3d}\right]$$

where x = the percentage (or number) of terminal units [%], a = unbranched chain elements [%], b = single branched chain elements [%], c = double branched chain elements [%], and d = triple branched chain elements [%].

Scheme 5. Principles of Methylation Analysis for an Exemplary Galactose Octamer[a]

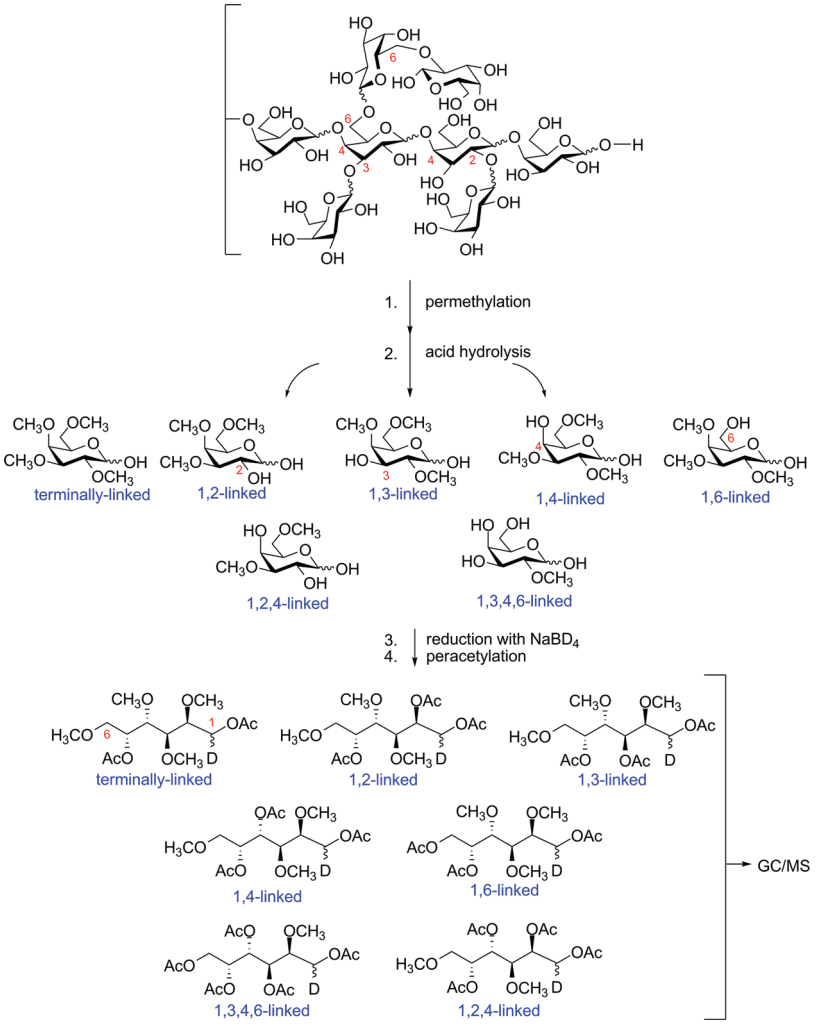

[a] The resulting alditol acetates are separated and quantified by GC, followed by fingerprint ID using their characteristic MS fragmentation.

Scheme 6. Linkage-Type Distribution of Anionic Self-Glycosylation of Glucopyranosyl Fluoride 5[a]

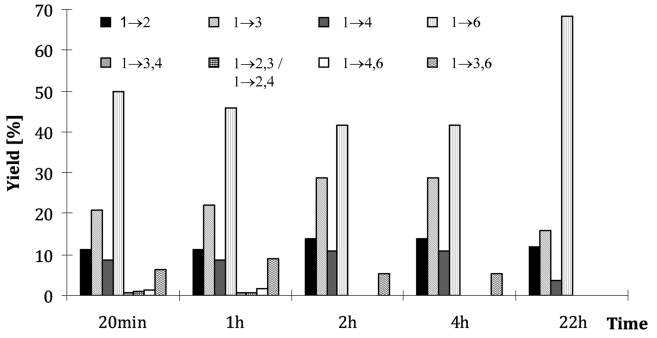

[a] Methylation analysis in time using GC/MS of the corresponding methylated alditol acetates after base promoted formation (1 equiv of lithium hydride, 40 °C) of *gluco*-oligomers.

Scheme 7. Average Chain Length $\overline{CL}$ for the Homooligomerization of α-D-Glucopyranosyl Fluoride 5 at 40 °C Sampled over 22 h, Based on the Results for the Methylation and GC/MS Linkage Analysis Data

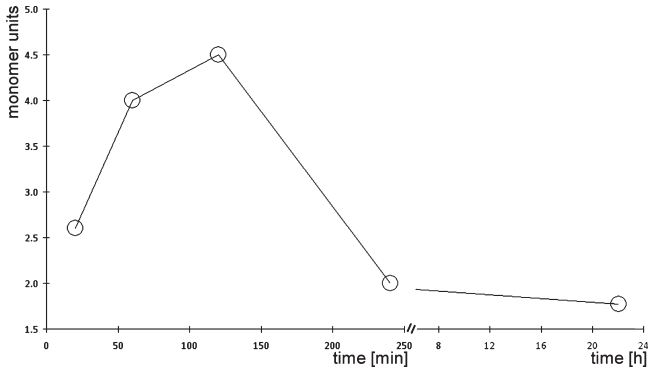

Using this formula, an *average chain length* of 9.33 building blocks is calculated:

$\overline{CL}$ for model structures in Figure 2:

$$\left[\frac{28}{11-3-2-3}\right] = \left[\frac{28}{3}\right] = 9.33$$

When applying these methylation analytics to above example mixture, the same ratios of relative percentage values are obtained, since relative percentage means the linkage distribution over all molecules present in the mixture. Therefore, it can be used in the formula, resulting in the same value for the model structure in Figure 2:

$$\overline{CL} = \left[\frac{100}{39.28-10.71-7.14-10.71}\right] = \left[\frac{100}{10.72}\right] = 9.33$$

The *average chain length* $\overline{CL}$ appears to be a useful indicator for the progression of the homooligomerization, and it allows insights into structural features and reactivity preferences. Based on these considerations, $\overline{CL}$ for the self-glycosylation of α-D-glucopyranosyl fluoride over time was calculated (Scheme 7).

Scheme 7 shows that the highest average length was obtained after 2 h consisting of 4.5 monomer units and then steadily decreases to an average of di- to trimers. This result indicates that the stability of polymers of increasing chain length is lower toward prolonged exposure to base conditions.

Since the highest average chain length was observed after 2 h for glucopyranosyl fluoride, other glycopyranosyl fluorides were tested using the same conditions. Additionally, two base conditions with 1 or 2 equiv of LiH were used, and the reaction was stopped after 2 h, corresponding to the maximal chain length observed in the *gluco* case. A summary of the linkage analysis is shown for each linkage type in Scheme 8 for *gluco*-, *galacto*-, *manno*-, and *fuco*pyranosyl oligomers.

Scheme 8. Base-Promoted Homooligomerization of Glycopyranosyl Fluorides 5−8[a]

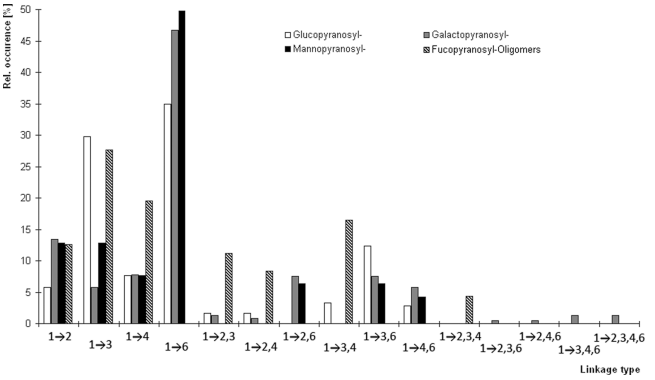

[a] Results of the linkage analysis by methylation and GC/MS for the anionic oligomerization of *glucopyranosyl*, *galactopyranosyl*, *mannopyranosyl*, and *fucopyranosyl* oligomers using 1 equiv of LiH for 2h at 40 °C. An increase in branching appears to be an indicator for higher reactivity and an increasing polymer size.

Scheme 9. Average Oligomer Chain Length $\overline{CL}$ Employing 1 and 2 equiv of LiH at 40 °C[a]

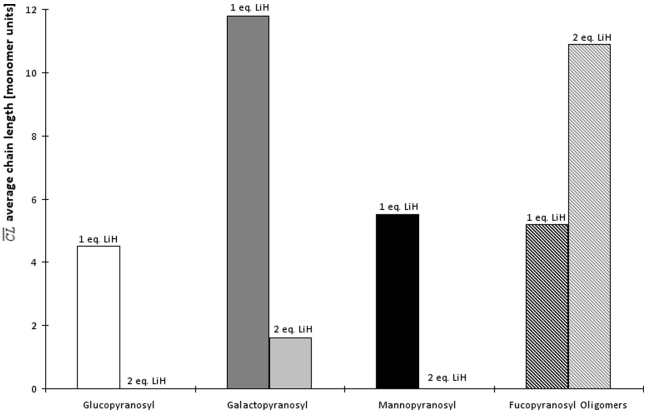

[a] Results obtained by methylation analysis.

In the case of the hexopyranoses the hydroxyl group in position 6 is the most reactive. The difference in reactivity of secondary hydroxyl groups is significantly lower, except for the glucose case. Here the hydroxy group in position 2 is more reactive than the others. A reason for this could be an activation by a hydrogen bridge between the hydroxyl group in position 2 and the α-anomeric oxygen. Surprisingly, galactopyranose forms the highest branched polymers. Apparently, the axial hydroxy group in position 4 is of corresponding reactivity as the generally more reactive equatorial ones.

Scheme 9 shows the average polymer length observed for 1 and 2 equiv of base based on linkage analysis. Only for fucopyranosyl oligomers the higher base concentration seems to promote the oligomerization; in all other cases, either no reaction took place or the average length dropped due to a decreased stability or solubility of the polymer.

The relative number of hydroxyl groups in the polymer increases by factors 3 or less depending on the degree of branching. Additionally, when increasing the base concentration, deprotonation leads to lower solubility due to generation of

Scheme 10. Deduced Average Structural Elements for *Fuco*- (2 equiv of LiH), *Galacto*- (1 equiv of LiH), *Gluco*- (1 equiv of LiH), and *Mannopyranosyl* (1 equiv of LiH) Oligomers

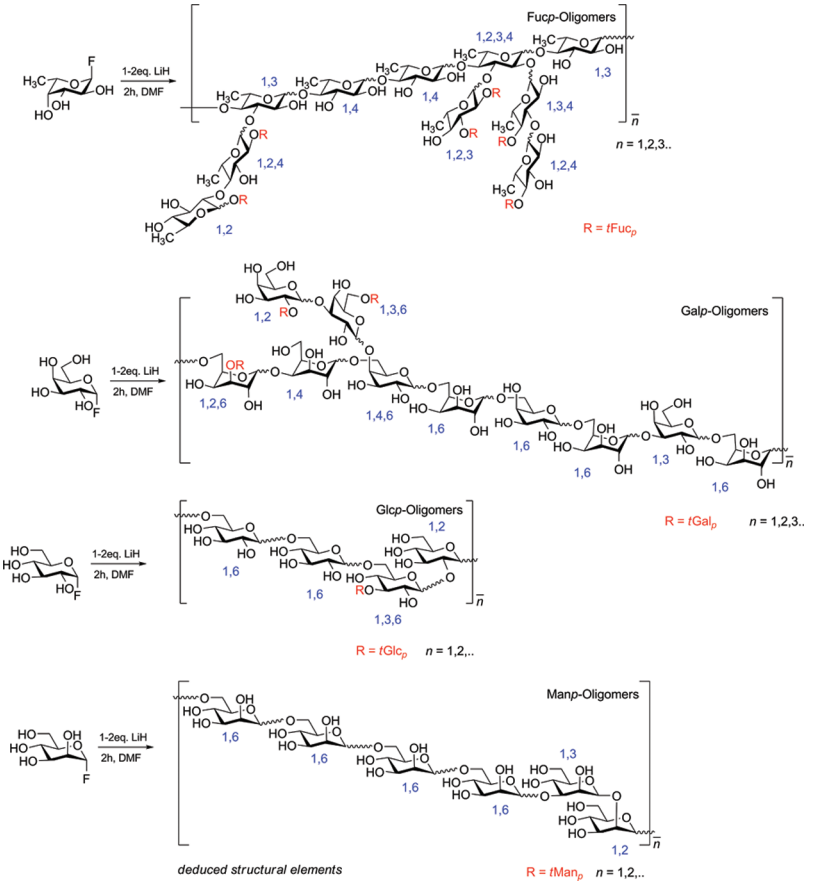

presumably multiply charged species. In case of the fucosides, both the methyl group at C-6 and the reduced number of hydroxyl groups might allow for a higher solubility in DMF. As shown in Scheme 8, the fucopyranoside and galactopyranoside oligomers tend to branch to a larger extent compared to gluco- and mannopyranoside. At enhanced deprotonation the above-mentioned higher solubility counteracts the charge, leading overall to a 2-fold increase in oligomer length (5.2 monomers when using 1 equiv of LiH and 10.9 monomer units when using 2 equiv of LiH).

In order to test the polymer stability toward the applied reaction conditions, a double pass glycosylation was performed. Thus, after the first pass the reaction was stopped at conditions found to generate the *highest average chain length* $\overline{CL}$. In a second self-oligomerization step the oligomer chains were then re-exposed using less forcing or similar base conditions. In order to screen for higher oligomers in addition to linkage analysis, gel permeation chromatography (GPC) was performed. The $\overline{CL}$ value stayed approximately the same, indicating that oligomer solubility is reduced or the stability of potentially generated higher polymers formed does not sustain such base conditions. The observed molar mass distribution was in the range of M_w 2000−3000 for single- and double-pass oligomerization, whereby a slight depolymerization is found as shown by GPC (Figure 3). The slight depolymerization was not further quantified or investigated. However, prolonged exposure to such harsh base conditions might degrade the oligomers to some extend. Additionally, an increasing oligomerization (and branching) likely leads to a reduced solubility.

Based on linkage analysis and the average chain length calculation, information about an averaged structural element of the formed oligomer(s) can be deduced (Scheme 10).

Recently, Kanzawa et al. demonstrated a thermal solid state polycondensation at temperatures of 110−180 °C, leading to highly branched β-linked polysaccharides.[21]

From a mechanistic point of view the regiospecific of solution phase glycosylation in DMF using glycopyranosyl fluorides is uncertain, since both α- and β-species were detected. However, solution phase conditions offer enhanced possibilities for fine-tuning to take advantage of positional differences in reactivity and for controlled reaction mechanism. Functionalization and protecting group chemistry of e.g. partly protected glycosyl fluorides to enhance solubility and chemical flexibility is under current investigation.

Conclusion

A novel glycosylation methodology for base-promoted single step self-oligomerization was established providing a direct route to complex glycosides. Employing four different glycosyl fluorides led to oligomers of ∼10−25 saccharide units. Each homooligomeric product mixture was analyzed qualitatively and quantitatively using a GC/MS linkage analysis of the corresponding methylated alditol acetates and Maldi-TOF. A numerical model was derived using the analytical data for the calculation of an average structural element of homooligomers drawing a detailed picture of prominent structure and their extent of branching. Functional design of glycoside based novel biodegradable materials is a prospective challenge. Starting point for optimization and reaction control is envisioned by reducing the polyfunctionality of carbohydrates using suitably functionalized building blocks.

Experimental/Materials and Methods

General Methods (GM). *GM1. Oligomerization Using Glycopyranosyl Fluorides.* Glycopyranosyl fluoride 1.00 g (5.5 mmol)

under a nitrogen or argon atmosphere was dissolved at 0 °C using dry *N*,*N*-dimethylformamide (20 mL) and suspended using lithium hydride (1 equiv). The mixture was stirred for 1 h at 0 °C under reduced pressure (~22 mbar) until hydrogen evolution ceased. The vacuum was released, and the flask flushed with nitrogen, followed by stirring for 2 h at 40 °C. The solution was neutralized using a mixed bead ion exchanger (Ion exchanger V, Merck) and filtered, and the solvent was removed under vacuum at 40 °C. The raw product was dissolved in deionized water and lyophilized. A small portion of the sample was homogenized by spatula. The substance was permethylated according to GM3 and MALDI-TOF-MS analysis performed.

GM2. Peracetylation Using Pyridine and Acetic Acid Anhydride. The starting material was dissolved in an excess of pyridine approximately 20-fold and then cooled to 0 °C prior to the addition of acetic acid anhydride (5 equiv) for each hydroxyl group while stirring. After the entire volume of acetic acid anhydride was added the cooling was removed. After completion of the reaction, the solvent was removed under vacuum, and the raw product was codistilled with toluene to remove pyridine. Purification was done either by flash column chromatographic purification or recrystallization from ethanol.

GM3. Methylation Analysis. The peracetylated saccharide mixture (20 mg) was dissolved in dry methanol (10 mL) and suspended with a spatula of sodium methanolate to adjust pH ~8. The solution was stirred overnight, followed by neutralization using Dowex 50 (H^+-form) and then filtered, and the solvent was removed under vacuum. The residue was taken up in DMSO (20 mL) and methyl iodide (1 mL) added, followed by sodium hydroxide (50%, 4 mL) and stirred at rt. After 30 min the solution was diluted with deionized water (20 mL) and extracted three times using dichloromethane. The combined organic phases were washed with water and then dried using sodium sulfate. Under mild vacuum the majority of the solvent was removed and carefully dried using a blown nitrogen stream. A portion of 10 mg of the residue is treated with trifluoroacetic acid (5 mL, 2.5 N) and heated for 1 h at 120 °C using a microwave reactor. The solution is dried in nitrogen air stream and codistilled twice using dry acetonitrile. The residue was taken up into sodium borodeuteriohydride (40 mg), ammonia solution (0.27 mL, 25%), and deionized water (1.73 mL of 0.5 M $NaBD_4$ in 2 M NH_3 solution).

The solution was stirred for 1 h at 60 °C, followed by an addition of acetone (2 mL) and stirring for an additional 20 min. To the solution acetonitrile (5 mL) was added, and the mixture was dried in a nitrogen air stream and this step repeated once. The residue was dissolved in glacial acetic acid (2 mL) and was suspended with ethyl acetate (1 mL) and acetic acid anhydride (3 mL) and shaken, and perchloric acid (0.1 mL) was added. The solution was stirred for 5 min and then cooled to 0 °C, and deionized water (10 mL) and 1-methylimidazole (0.2 mL) were added and stirred for an additional 5 min at this temperature. The phase was extracted by addition of dichloromethane (1 mL), and the flask was shaken vigorously. After phase separation, the dichloromethane layer was carefully pipetted off and was kept at −26 °C for GC/MS analyses.

GC MS was done on a HP 6890, using a HP-5 column (30 m), with an inner diameter (i.d.) of 0.32 mm and film thickness (f.th.) of 0.25 μm with H_2 as a carrier gas. Temperature program (oven): 40 °C for 2 min, 30°/min up to 60 °C, then 5°/min up to 300 °C. Temperature programmable injector (PTV); 50 °C for 0.2 min, 300°/min up to 250 °C. Detector type: flame ionization detector (FID) (Figure 1).

GM4. Preparation of Peracetylated Glycopyranosyl Fluorides. The reaction was performed in a sealed plastic vial. 10 mmol of the starting peracetylated pentaacetate was dissolved in HF/pyridine (10 mL, 70%) solution and stirred for 4 h at rt. The reaction was monitored by TLC (ethyl acetate/petrol ether 1:1). After completion of the reaction, the solution was diluted with dichloromethane (30 mL) and deionized water (30 mL). Excess acid was neutralized by addition of sodium carbonate until no gas evolution was visible, and the pH was adjusted slightly above pH ~7. The organic phase was separated, the aqueous layer was extracted three times using dichloromethane, and the combined organic phases were dried using sodium sulfate and filtered, and the solvent was removed under vacuum. The raw product was purified by flash column chromatography (ethyl acetate/petrol ether 1:2).

GM5. Preparation of Glycopyranosyl Fluorides. The peracetylated product was deacetylated under Zemplén conditions, using a solution of methanolate in methanol (pH 8.5) at 0 °C while stirring for 2 h under TLC control (ethyl acetate/petrol ether 3:1). After completion the solution was neutralized using ion-exchange resin (Dowex 50, H^+-form) and filtered, and the solvent was removed under vacuum. No further purification was done.

MALDI-TOF-MS. Matrix-assisted laser desorption ionization time-of-flight mass spectrometric analysis (MALDI-TOF MS) were performed on a Bruker Biflex III, positive mode (matrix: 2,5-dihydroxybenzoic acid (DHB).

Gel Permeation Chromatography (GPC). GPC was done at room temperature using a multiangle light scattering and concentration detection TSK-Gel PWXL G3000, G4000, G5000, and G6000 columns (Toso Haas, Stuttgart, Germany) in decreasing pore size were coupled online to a multiangle light scattering (MALS) detector Dawn DSP (Wyatt Technology, Santa Barbara, CA) and a differential refractive index detector (dRI) Optilab DSP (Wyatt Technology). Data acquisition and processing was performed using Astra 4 software (Wyatt Technology, Santa Barbara, CA). Flow rate was maintained at 0.5 mL/min using a Constametric 3500 pump. The GPC refractogram for glucopyranosyl oligomers is plotted as molar mass (or detector response) vs elution volume showing a distribution of $M_w \sim 2000-3000$.

2,3,4,6-Tetra-O-acetyl-α-D-glucopyranosyl Fluoride [*1*]. Preparation according to GM4. $C_{14}H_{19}O_9F$ (350.30 g/mol); $[\alpha]_{546}^{20} = +80$ (*c* 1, $CHCl_3$). Lit.:[22] $[\alpha]_D^{25} = +91$ (*c* 1.1, $CHCl_3$); mp 100 °C. Lit.:[23] 112 °C; colorless solid. Yield: 70%. ^{1}H NMR (400 MHz, $CDCl_3$): δ = 5.74 (d, 1H, H-1), 5.41 (vt, 1H, H-3), 5.13 (vt, 1H, H-4), 4.96 (dd, 1H, H-2), 4.27 (vt, 1H, H-6a), 4.14 (dd, 1H, H-5, H-6b), 2.03, 2.02, 1.97, 1.92 ppm (CH_3). $J_{1,2} = 2.8$, $J_{2,3} = 10.0$, $J_{3,4} = 10.2$, $J_{4,5} = 10.1$, $J_{5,6a} = 4.6$, $J_{5,6b} = 2.4$, $J_{6a,6b} = 12.5$, $J_{1,F} = 53.0$, $J_{2,F} = 25.0$ Hz. ^{13}C NMR (100 MHz, $CDCl_3$): δ = 170.00, 170.00, 169.66, 169.84, (CO), 103.61 (C1), 70.00 (C2), 69.64 (C5), 69.57 (C3), 67.15 (C4), 61.0 (C6), 20.50, 20.55, 20.25, 20.31 ppm (CH_3). $J_{C1,F} = 228$, $J_{C2,F} = 24$ Hz.

2,3,4,6-Tetra-O-acetyl-α-D-galactopyranosyl Fluoride [*2*]. Preparation according to GM4. $C_{14}H_{19}O_9F$ (350.30 g/mol); $[\alpha]_D^{20} = +100°$ (*c* 1, $CHCl_3$). Lit.:[11,23] $[\alpha]_D^{20} = +96.5°$ (*c* 1, $CHCl_3$); mp 62 °C. Lit.:[23] 67−68 °C; colorless solid. Yield: 68%. ^{1}H NMR (400 MHz, $CDCl_3$): δ (ppm) = 5.74 (dd, 1H, H-1), 5.46 (d, 1H, H-4), 5.29 (dd, 1H, H-3), 5.12 (ddd, 1H, H-2), 4.34 (vt, 1H, H-5), 4.08 (m, 2H, H-6a. H-6b) 2.09, 2.05, 1.99, 1.94 (CH_3). $J_{1,2} = 2.8$, $J_{2,3} = 11.0$, $J_{3,4} = 3.4$, $J_{5,6a} = 6.6$, $J_{5,6b} = 6.6$, $J_{1,F} = 53.3$, $J_{2,F} = 23.6$ Hz. ^{13}C NMR (100 MHz, $CDCl_3$): δ (ppm) = 174.34, 172.98, 172.85, 171.02 (CO), 104.72 (C-1), 69.27 (C-5), 67.95 (C-3), 67.76 (C-4), 67.40 (C-2), 61.67 (C-6), 21.06, 21.03, 21.00, 20.94 (CH_3). $^1J_{C1,F} = 113.6$ Hz.

2,3,4,6-Tetra-O-acetyl-α-D-mannopyranosyl Fluoride [*3*]. Preparation according to GM4. $C_{14}H_{19}O_9F$ (350.30 g/mol); $[\alpha]_D^{20} = +7$ (*c* 1, $CHCl_3$); mp 115 °C. Lit.:[24] 67−68 °C; $[\alpha]_{546}^{20} = +29$ (*c* 1, $CHCl_3$). Lit.:[24] $[\alpha]_D^{20} = +22$ (*c* 1.68, $CHCl_3$); colorless syrup. Yield: 65%. ^{1}H NMR (400 MHz, $CDCl_3$): δ (ppm) = 5.55 (d, 1H, H-1), 5.40−5.30 (m, 3H, H-2, H-3, H-4), 4.14 (m, 2H, H-6a, H-6b), 2.01, 1.98, 1.98, 1.97 (CH_3). $J_{1,2} = 1.7$, $J_{1,F} = 48.3$ Hz. ^{13}C NMR (100 MHz, $CDCl_3$): δ (ppm) = 104.01 (C1), 72.73 (C5), 68.37 (C3), 66.62 (C2), 66.15 (C4), 62.51 (C6), 20.58, 20.05, 19.95, 19.56 (CH_3). *C*O signals were not resolved due to the low signal intensity. $J_{C1,F} = 220$, $J_{C2,F} = 24$ Hz.

2,3,4-Tri-O-acetyl-α-D-fucopyranosyl Fluoride [***4***]. Preparation according to GM4. $C_{12}H_{17}FO_7$ (292.09 g/mol); $[\alpha]_D^{20}$ = +100° (*c* 1, $CHCl_3$). Lit.:[11] $[\alpha]_D^{20}$ = +148° (*c* 0.4, $CHCl_3$); mp 84 °C; colorless solid. Yield: 36%. ^{1}H NMR (400 MHz, $CDCl_3$): δ (ppm) = 5.76 (dd, 1H, H-1), 5.39−5.35 (m, 2H, H-3, H-4), 5.17 (ddd, 1H, H-2), 4.35 (vt, 1H, H-5), 2.17, 2.11, 2.01, (CH_3), 1.20 (d, 3H, H-6). $J_{1,2}$ = 2.5, $J_{2,3}$ = 10.8, $J_{4,5}$ < 1, $J_{5,6}$ = 6.6, $J_{1,F}$ = 53.8, $J_{2,F}$ = 24.0 Hz. ^{13}C NMR (100 MHz, $CDCl_3$): δ (ppm) = 104.55 (C1), 70.38, (C4), 67.61 (C5), 67.45 (C-2), 67.36 (C3), 20.70, 20.64, 20.58 ($COCH_3$), 15.79 (C-6). *C*O signals could not be assigned due to the low signal intensity. $J_{C1,F}$ = 181, $J_{C2,F}$ = 12 Hz.

α-*D*-*Glucopyranosyl Fluoride* [***5***]. Preparation according to GM5. $C_6H_{11}FO_5$ (182.15 g/mol); mp 115 °C. Lit.:[23] 112−119 °C; $[\alpha]_{546}^{20}$ = +77 (*c* 1, H_2O). Lit.:[25] $[\alpha]_D^{25}$ = +90 (*c* 1, H_2O); colorless solid. Yield: quantitative. ^{1}H NMR (400 MHz, D_2O): δ = 5.63 (dd, 1H, H-1), 3.87−3.54 (m, 4H, H-2, H-3, H-4, H-5), 3.50−3.38 ppm (m, 2H, H-6a, H-6b). $J_{1,2}$ = 2.8, $J_{1,F}$ = 53.0, $J_{2,F}$ = 24.1 Hz. ^{13}C NMR (100 MHz, D_2O): δ = 107.71 (C1), 74.52, (C3), 71.38 (C2), 72.67, 68.92 (C-4, C-5), 60.52 ppm (C-6). $J_{C1,F}$ = 222, $J_{C2,F}$ = 25 Hz.

α-*D*-*Galactopyranosyl Fluoride* [***6***]. Preparation according to GM5. $C_6H_{11}FO_5$ (182.15 g/mol); $[\alpha]_D^{20}$ = +122 (*c* 1, MeOH). Lit.:[25] $[\alpha]_D^{20}$ = +127 (*c* 1, MeOH); mp 114 °C; colorless solid. Yield: quantitative. ^{1}H NMR (400 MHz, D_2O): δ (ppm) = 5.42 (dd, 1H, H-1), 4.98 (d, 1H, H-4), 4.56 (ddd, 1H, H-2), 3.67 (vt, 1H, H-3), 3.55 (m, 1H, H-5), 3.41 (m, 2H, H-6a, H-6b). $J_{1,2}$ = 2.8, $J_{2,3}$ = 9.1, $J_{3,4}$ = 3.8, $J_{4,5}$ < 1, $J_{1,F}$ = 54.7, $J_{2,F}$ = 24.1 Hz. ^{13}C NMR (100 MHz, D_2O): δ (ppm) = 108.62 (C1), 74.30, (C5), 74.27 (C4), 69.41 (C-3), 68.12 (C-2), 14.93 (C-6). $J_{C1,F}$ = 222, $J_{C2,F}$ = 23 Hz.

α-*D*-*Mannopyranosyl Fluoride* [***7***]. Preparation according to GM5. $C_6H_{11}FO_5$ (182.15 g/mol); $[\alpha]_{546}^{20}$ = +27 (*c* 1, $CHCl_3$). Lit.[26] $[\alpha]_D^{20}$ = +16 (*c* 1, H_2O); colorless syrup. Yield: quantitative. ^{1}H NMR (400 MHz, D_2O): δ (ppm) = 5.42 (d, 1H, H-1), 3.90 (s, 1H, H-3), 3.72 (m, 1H, H-2), 3.50−3.40 (m, 3H, H-4, H-6a, H-6b), 3.25 (m, 1H, H-5). $J_{1,2}$ = 1.0, $J_{1,F}$ = 49.3 Hz. ^{13}C NMR (100 MHz, D_2O): δ = 103.19 (C1), 77.32 (C5), 75.30 (C3), 71.22 (C2), 68.20 (C4), 61.95 ppm (C6). $J_{C1,F}$ = 220, $J_{C2,F}$ = 24 Hz.

α-*D*-*Fucopyranosyl Fluoride* [***8***]. Preparation according to GM5. $C_6H_{11}FO_4$ (166.15 g/mol); $[\alpha]_D^{20}$ = +139 (*c* 1, MeOH). Lit.:[11] $[\alpha]_D^{20}$ = +137° (*c* 1, MeOH); mp 235 °C; colorless solid. Yield: quantitative. ^{1}H NMR (400 MHz, D_2O): δ (ppm) = 5.60 (dd, 1H, H-1), 5.13 (d, 1H, H-4), 4.21 (vt, 1H, H-3), 3.84 (ddd, 1H, H-2), 3.79 (m, 1H, H-5), 1.13 (d, 3H, H-6). $J_{1,2}$ = 3.5, $J_{2,3}$ = 10.1, $J_{3,4}$ = 3.8, $J_{4,5}$ < 1, $J_{5,6}$ = 6.6, $J_{1,F}$ = 54.1, $J_{2,F}$ = 24.0 Hz. ^{13}C NMR (100 MHz, D_2O): δ (ppm) = 97.63 (C1), 73.33, (C4), 72.29 (C5), 71.84 (C-2), 69.67 (C-3), 14.93 (C-6). *C*O signals not visible due to low signal intensity. $J_{C1,F}$ = 182, $J_{C2,F}$ = 12 Hz.

Acknowledgment. Support for this work by the DFG and FCI is gratefully acknowledged.

References and Notes

(1) Mukaiyama, T.; Murai, Y.; Shoda, S. *Chem. Lett*. **1981**, *6*, 431–432.
(2) Yu, B.; Li, B.; Xing, G.; Hui, Y. *J. Comb. Chem*. **2001**, *3*, 404–406.
(3) Kanie, O.; Barresi, F.; Ding, Y.; Labbe, J.; Otter, A.; Forsberg, L. S.; Ernst, B.; Hindsgaul, O. *Angew. Chem., Int. Ed. Engl*. **1996**, *34*, 2720–2722.
(4) Kobayashi, S.; Ohmae, M. *Adv. Polym. Sci*. **2006**, *194*, 159–210.
(5) Toshima, K. *Carbohydr. Res*. **2000**, *327*, 15–26.
(6) Kreuzer, M.; Thiem, J. *Carbohydr. Res*. **1986**, *149*, 347–361.
(7) Kunz, H.; Sager, W. *Helv. Chim. Acta* **1985**, *68*, 283–287.
(8) Micheel, F.; Klemer, A. *Adv. Carbohydr. Chem*. **1961**, *16*, 85–103.
(9) Hagemann, H., Klamann, D., Eds. In *Methoden der Organischen Chemie*; Houben-Weyl: Thieme Stuttgart, 1992; Bd. E14a/3, pp 621−651.
(10) Thiem, J.; Fritsche-Lang, W.; Schlingmann, M.; Deger, H.-M.; Kreuzer, M. Ger. Offen. DE 34 26 074 (14.7.1984; 22.1.1986); *Chem. Abstr*. **1986**, *105*, 191564f; EP 0 168 723 B1 (5.7.1985; 7.3.1990).
(11) Schröder, S. Dissertation, Hamburg, **2003**.
(12) Steinmann, A.; Thimm, J.; Thiem, J. *Eur. J. Org. Chem*. **2007**, *33*, 5506–5513.
(13) Steinmann, A.; Thimm, J.; Wollik, N.; Thiem, J. *Curr. Org. Chem*. **2008**, *12*, 1010–1020.
(14) Schmidt, R. R.; Reichrath, M.; Moering, U. *J. Carbohydr. Chem* **1984**, *3*, 67–84.
(15) Zhu, X.; Schmidt, R. R. *Angew. Chem., Int. Ed*. **2009**, *48*, 1900–1934.
(16) Bjorndal, H.; Lindberg, B.; Svensson, S. *Carbohydr. Res*. **1967**, *5*, 433–40.
(17) Harris, P. J.; Henry, R. J.; Blakeney, A. B.; Stone, B. A. *Carbohydr. Res*. **1984**, *127*, 59–73.
(18) Hoelter, D.; Burgath, A.; Frey, H. *Acta Polym*. **1997**, *48*, 30–35.
(19) Frey, H.; Hoelter, D. *Acta Polym*. **1999**, *50*, 67–76.
(20) Satoh, T.; Imai, T.; Ishihara, H.; Maeda, T.; Kitajyo, Y.; Narumi, A.; Kaga, H.; Kaneko, N.; Kakuchi, T. *Macromolecules* **2003**, *36*, 6364–6370.
(21) Kanzawa, A.; Namiki, S.; Suzuki, M. *J. Polym. Sci., Part A: Polym. Chem*. **2007**, *45*, 3851–3860.
(22) Igarashi, K.; Honma, T.; Irisawa, J. *Carbohydr. Res*. **1970**, *13*, 49–55.
(23) Horneman, A. M.; Lundt, I. *J. Carbohydr. Chem*. **1995**, *14*, 1–8.
(24) Miethchen, R.; Hager, C.; Hein, M. *Synthesis* **1997**, *2*, 159–161.
(25) Barnett, J. E. G. *Carbohydr. Res*. **1969**, *9*, 21–31.
(26) Micheel, F.; Borrmann, D. *Chem. Ber*. **1960**, *93*, 1143–1147.